

EPJ B

Condensed Matter
and Complex Systems

EPJ.org
your physics journal

Eur. Phys. J. B (2013) 86: 403

DOI: [10.1140/epjb/e2013-40509-1](https://doi.org/10.1140/epjb/e2013-40509-1)

Percolation of polyatomic species on a simple cubic lattice

G.D. Garcia, F.O. Sanchez-Varretti, P.M. Centres and A.J. Ramirez-Pastor

 edp sciences



 Springer

Percolation of polyatomic species on a simple cubic lattice

G.D. Garcia¹, F.O. Sanchez-Varretti¹, P.M. Centres^{2,a}, and A.J. Ramirez-Pastor²

¹ Universidad Tecnológica Nacional, Facultad Regional San Rafael, Gral J.J. De Urquiza 340, C.P. M5602GCH, San Rafael, Mendoza, Argentina

² Departamento de Física, Instituto de Física Aplicada, Universidad Nacional de San Luis-CONICET, Ejército de los Andes 950, D5700BWS, San Luis, Argentina

Received 20 May 2013 / Received in final form 23 July 2013

Published online 25 September 2013 – © EDP Sciences, Società Italiana di Fisica, Springer-Verlag 2013

Abstract. In the present paper, the site-percolation problem corresponding to linear k -mers (containing k identical units, each one occupying a lattice site) on a simple cubic lattice has been studied. The k -mers were irreversibly and isotropically deposited into the lattice. Then, the percolation threshold and critical exponents were obtained by numerical simulations and finite-size scaling theory. The results, obtained for k ranging from 1 to 100, revealed that (i) the percolation threshold exhibits a decreasing function when it is plotted as a function of the k -mer size; and (ii) the phase transition occurring in the system belongs to the standard 3D percolation universality class regardless of the value of k considered.

1 Introduction

The percolation problems have been attracting a great deal of interest for several decades, and the activity in this field is still growing [1–25]. It settles the basis to the understanding of the behavior of many systems such as network theory [3,8,9,13], transport and flow in porous media [3–5], transport in disordered media [14,15], spread of disease in populations [16], forest fire propagation [17], simulated spread fire in multi-compartmented structures [18], spread of the computer virus [19], network failures [20], formation of gels [21]. They are just a few examples of the wide applicability of percolation, also known as percolation theory.

The first mathematical formulation of classical percolation threshold was that of Broadbent and Hammersley [26,27]. They exposed concepts that nowadays are widely used, representing the flow of fluid through porous media by a simplified *lattice percolation model*. In addition, the authors were able to prove that their model has a percolation threshold. To illustrate this percolation threshold, we shall describe the stages of the percolation problem on a lattice of sites which are occupied with probability p or empty (nonoccupied) with probability $(1-p)$. Nearest-neighboring occupied sites form structures called clusters. Quantities relevant to percolation will depend on the concentration of sites and geometry of the lattice.

When the concentration is low, the sites appear singly or in small isolated clusters of adjacent elements. As p increases, the mean size of the clusters increases monotonically. When the occupation probability exceeds a critical value (called the percolation threshold p_c), a macroscopic,

spanning, or an infinite cluster, occupying a finite fraction of the total number of sites, emerges. The percolation threshold can be depicted as the concentration of sites for which a complete path of adjacent sites crossing the entire system becomes possible. The percolation transition is then a geometrical phase transition where the critical concentration separates a phase of finite clusters ($p < p_c$) from a phase where an infinite cluster is present ($p > p_c$). This transition is a second-order phase transition and can be characterized by well-defined critical exponents.

One may also consider a percolation problem in which both sites and bonds are independently occupied, with occupancy fractions p_s and p_b , respectively. This more general model, known as the site-bond percolation model [28], has been widely used to study the phenomenon of polymer gelation [29].

Most studies are devoted to *single occupied site* (bond) on different lattices (like square, triangular, simple cubic, face centered cubic, and many others) in the framework of Monte Carlo (MC) analysis. On the other hand, there have been a few studies focused on generalizing the pure percolation model by including deposition of elements occupying more than one site (bond) [30–40].

In reference [31] is shown (by studying the multiple-site percolation problem) that p_c exhibits an exponentially decreasing behavior as a function of the k -mer size. This feature was observed both for straight rigid k -mers and tortuous k -mers isotropically deposited on 2D square lattices. In all the studied cases, the problem was shown to belong to the random percolation universality class. Nevertheless, in a recent work by Tarasevich et al. [40] a different behavior was found for the percolation threshold: namely a non-monotonic k -mer size dependence.

^a e-mail: pcentres@unsl.edu.ar

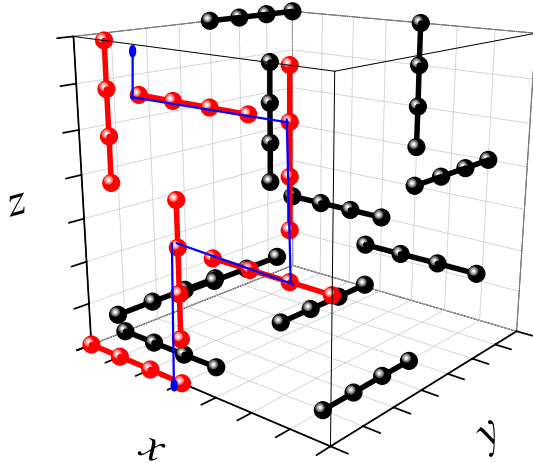


Fig. 1. Schematic representation of a simple cubic lattice in which some k -mers ($k = 4$) have been deposited; for sake of simplicity the lattice site are not shown. A percolation path is indicated with a blue line on the red k -mers, which are percolating in the z -direction.

In this context, the present paper deals with the percolation of straight rigid k -mers on a simple cubic lattice. Using MC simulations and a detailed finite-size scaling analysis, the main percolation properties are studied. The main objectives of the paper are (i) to determine the dependence of the percolation threshold on the size of the deposited k -mers and (ii) to discuss the universality class of the phase transition. This work is also motivated by the particular behavior reported in reference [40]. The only study on these systems has been reported for dimers (k -mers with $k = 2$) in reference [39].

The paper is organized as follows. In Section 2, the basis of the model for the deposition of the k -mers on the simple cubic lattice is presented. In Section 3, finite-size scaling analysis of MC simulations is carried out. In Section 4, the dependence of the percolation threshold on the k -mer size is discussed. Finally, in Section 5 conclusions are drawn.

2 Model and Monte Carlo simulation details

The following scheme is usually called standard model of deposition or Random Sequential Adsorption (RSA). Let us consider an initially empty simple cubic lattice of linear size L on which k -mers are randomly deposited. When the size of the k -mers is one (*monomers*), the procedure of deposition is as follows: a lattice site is chosen at random, if the selected site is unoccupied then the monomer is deposited, otherwise, the attempt is rejected. When $k > 1$ the process is as follows: (i) one of the three possible directions (x, y, z) and a starting site are randomly chosen; (ii) if, beginning at the chosen site, there are k empty sites, then a k -mer is deposited on those sites. Otherwise, the attempt is rejected. When N k -mers are deposited, the concentration is $p = \frac{kN}{L^3}$. In Figure 1, a typical final state generated by RSA is depicted.

As it was already mentioned, the central idea of percolation theory is based on finding the minimum concentration p for which a cluster extends from one side of the system to the opposite. This particular value of the concentration is called *critical concentration* or *percolation threshold* and determines a well defined phase transition in the system. We are interested in determining (i) how the percolation threshold is modified when the size of the k -mer is increased and (ii) what universality class the phase transition of this problem belongs to.

The finite-scaling theory gives us the basis to determine the percolation threshold and the critical exponents of a system with a reasonable accuracy. The probability $R = R_{L,k}^X(p)$ that a $L \times L \times L$ lattice percolates at the concentration p of occupied sites by k -mers of size k can be defined according to [3,41–43]. According to the last definition X , for our problem, can mean:

- $R_{L,k}^R(p)$: the probability of finding a rightward percolating cluster, along the x -direction;
- $R_{L,k}^D(p)$: the probability of finding a downward percolating cluster, along the z -direction;
- $R_{L,k}^F(p)$: the probability of finding a frontward percolating cluster, along the y -direction.

Other useful definitions for the finite-size analysis are:

- $R_{L,k}^U(p)$: the probability of finding a cluster which percolates on any direction;
- $R_{L,k}^I(p)$: the probability of finding a cluster which percolates in the three (mutually perpendicular) directions;
- $R_{L,k}^A(p) = \frac{1}{2}[R_{L,k}^U(p) + R_{L,k}^I(p)]$.

In order to express $R_{L,k}^X(p)$ as a function of continuous values of p , it is convenient to fit $R_{L,k}^X(p)$ with some approximating function through the least-squares method. The fitting curve is the *error function* because $dR_{L,k}^X(p)/dp$ is expected to behave like the Gaussian distribution [42,43]

$$\frac{dR_{L,k}^X}{dp} = \frac{1}{\sqrt{2\pi}\Delta_{L,k}^X} \exp\left\{-\frac{1}{2}\left[\frac{p - p_{c,k}^X(L)}{\Delta_{L,k}^X}\right]^2\right\}, \quad (1)$$

where $p_{c,k}^X(L)$ is the concentration at which the slope of $R_{L,k}^X(p)$ is the largest and $\Delta_{L,k}^X$ is the standard deviation from $p_{c,k}^X(L)$.

In addition to the different probabilities, the percolation order parameter ($P = \langle S_L \rangle / L^3$) [44,45] has been measured; where S_L represents the size of the largest cluster and $\langle \dots \rangle$ means an average over MC runs. The corresponding percolation susceptibility χ has also been calculated, $\chi = [\langle S_L^2 \rangle - \langle S_L \rangle^2] / L^3$.

MC simulations were applied to determine each of the previously mentioned quantities. Thus, each MC run consists of the following steps: (a) construction of a simple cubic lattice of linear size L , with a given coverage p , (b) perform the cluster analysis using the Hoshen and Kopelman algorithm [46]. In the last step, the size of largest cluster S_L is determined, as well as the existence of a percolating island. This spanning cluster, as was mentioned,

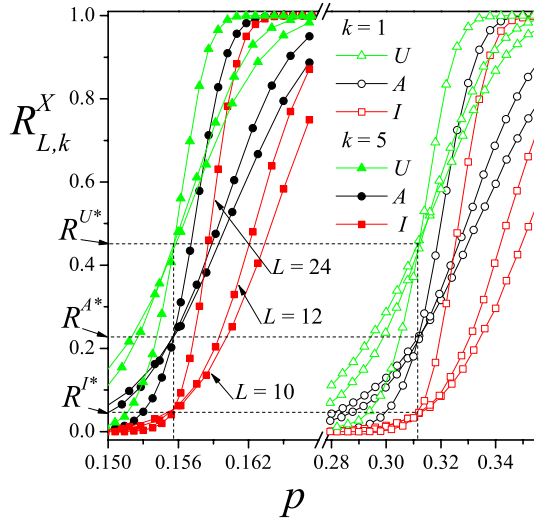


Fig. 2. Fraction of percolation lattices as a function of the concentration p defined as $p = kN/L^3$, where k is the k -mer size, N the number of deposited k -mers and L the lattice linear size.

could be R , D or F . At the same time I , U and A were determined.

For the above algorithm $n \sim 10^5$ runs were carried out for several values of the system size ($L/k = 6, 8, 10, 12, 24$). The L/k ratio is kept constant to prevent spurious effects due to the k -mer size in comparison with the lattice linear size L .

3 Results

In Figure 2, the probabilities $R_{L,k}^U(p)$, $R_{L,k}^I(p)$ and $R_{L,k}^A(p)$ are shown for two different values of k ($k = 1$ and $k = 5$ as indicated).

From a simple inspection of the figure (and from data not shown here for the sake of clarity) it is observed that: (a) the curves, corresponding to the various percolation criteria (R , D , F , etc.), cross each other in a unique universal point, R^{X*} , which depends on the criterion X used; (b) those points do not modify their numerical value for the different k used (ranged between $k = 1$ to $k = 100$); (c) those points are located at very well defined values in the p -axes determining the critical percolation threshold for each k and (d) p_c decreases for increasing k -mer sizes.

The probability $R_{L,k}^X(p)$ is also called in the literature the percolation cumulant, whose properties are identical to those of the Binder cumulant U_L in standard thermal transitions [41,47]. Namely, $R_{L,k}^X(p)$ obeys the same scaling relation as U_L , and the intersection of the curves of $R_{L,k}^X(p)$ for different system sizes can be used to determine the critical point that characterizes the phase transition occurring in the system [3,31,48–50]. From this perspective, the result given in point (b) could be taken as a preliminary indication that the universality class of the phase transition involved in the problem is conserved no matter the value of k . However, as pointed out by Selke

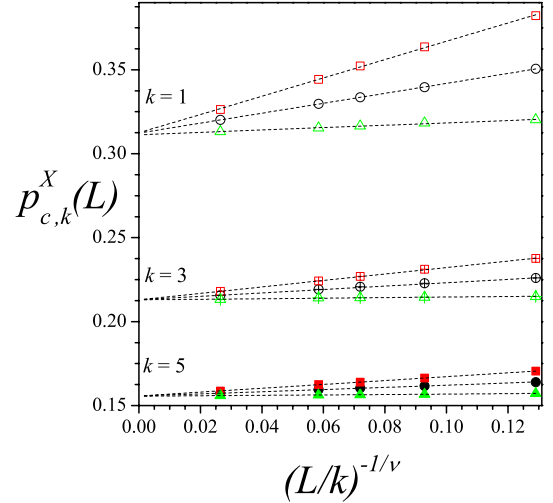


Fig. 3. Extrapolation of $p_{c,k}^X(L)$ towards the thermodynamic limit according to the theoretical prediction given by equation (3). Squares, circles and triangles: the values of $p_{c,k}(L)$ obtained by using the criteria I , A and U , respectively. Different values of k are presented as indicated.

and Shchur [51,52], the measure of the cumulant intersection may depend on various details of the model which do not affect the universality class, in particular, the boundary condition, the shape of the lattice, and the anisotropy of the system. Consequently, more research is required to determine the universality class of the phase transition.

For each $R_{L,k}^X(p)$ and $\frac{dR_{L,k}^X(p)}{dp}$ curve, the fitting function was determined by least mean-square method using equation (1). In this way, $p_{c,k}^X(L)$ is determined for the different values of k and L .

We extrapolate the previous results of $p_{c,k}^X(L)$ for $L \rightarrow \infty$ by using the finite-scaling hypothesis. Thus, the correlation length, ξ , associated with emergence of the percolation cluster, has the scaling relation:

$$\xi \propto |p - p_{c,k}|^{-\nu}, \quad (2)$$

where ν is the critical exponent. It is known [53] that $\nu = 7/8$ for random 3D percolation. As $p \rightarrow p_{c,k}^X(L)$ the correlation length $\xi \rightarrow L$, being L the linear dimension of the system. Thus, we have

$$p_{c,k}^X(L) = p_{c,k}^X(\infty) + A^X L^{-1/\nu}, \quad (3)$$

where A^X is a non-universal constant. Figure 3 shows the extrapolation towards the thermodynamic limit of $p_{c,k}^X(L)$ according to equation (3) for different values of k as indicated. This figure supports the relation given by equation (3): (a) all the curves (different criteria) are well correlated by a linear function, and (b) they have a quite similar value for the ordinate in the limit $L \rightarrow \infty$.

From the procedure shown in Figure 3, one obtains $p_{c,k}^X(\infty)$ for the criteria I , A and U . Combining the three estimates for each k , the final values of $p_{c,k}(\infty)$ are obtained. The maximum of the differences between

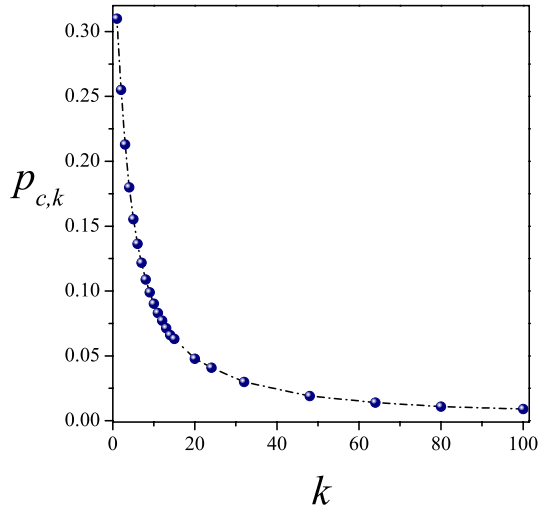


Fig. 4. The percolation threshold as a function of k . The error in each measurement is smaller than the size of the symbols.

$|p_{c,k}^I(\infty) - p_{c,k}^A(\infty)|$ and $|p_{c,k}^U(\infty) - p_{c,k}^A(\infty)|$ gives the error bar for $p_{c,k}(\infty)$.

In Figure 4 the percolation threshold $p_{c,k}(\infty)$ is plotted as a function of the k -mer size. The values for $k = 1$ [$p_{c,k=1}(\infty) = 0.3116077(4)$] and $k = 2$ [$p_{c,k=2}(\infty) = 0.2555(1)$] have been already reported in [39] and [54], respectively. The points corresponding to $k = 80$ and $k = 100$ were calculated for three relatively small values of L/k (4, 6, 8), with an effort reaching almost the limits of our computational capabilities. A compilation of the numerical values is also presented in Table 1.

For all the range of studied sizes, the percolation threshold decreases upon increasing k . This result contrasts with the one of Tarasevich et al. [40], who found that, for two-dimensional square lattices, the percolation threshold shows a nonmonotonic k -mer size dependence. Namely, the percolation threshold decreases for small particle sizes, goes through a minimum at $k \approx 13$, and finally monotonically increases as k increases. This nonmonotonic behavior observed in two dimensions has been explained accounting for the local alignment effects occurring for large values of k [40]. In the case of cubic lattices, the same effects are not detected in the range of values of k between 1 and 80.

In Figure 3 the value $\nu = 7/8$ was used. Nevertheless, the value of ν can be obtained through the scaling relationship for $R_{L,k}^X(p)$:

$$R_{L,k}^X(p) = \overline{R}_k^X \left[(p - p_{c,k}) L^{\frac{1}{\nu}} \right], \quad (4)$$

being $\overline{R}_k^X(u)$ the scaling function and $u \equiv (p - p_{c,k}) L^{\frac{1}{\nu}}$. Thus, the maximum of the derivative of equation (4) leads to $\left(\frac{dR_{L,k}^X}{dp} \right)_{max} \propto L^{\frac{1}{\nu}}$. In the inset of Figure 5, this relation has been plotted as a function of L/k (in log-log scale) for different k -mers as indicated. As it can be observed, the slopes of the curves ($1/\nu$) remain constant (and close to $8/7$) for all values of k . The results match,

Table 1. Compilation of the percolation thresholds for different k -mer sizes.

k -mer size, k	Percolation threshold, $p_{c,k}$
1	0.3116077(4) [46]
2	0.2555(1) [36]
3	0.2129(1)
4	0.1800(1)
5	0.1555(1)
6	0.1364(1)
7	0.1218(1)
8	0.1089(1)
9	0.0990(1)
10	0.0901(1)
11	0.0831(1)
12	0.0772(1)
13	0.0714(1)
14	0.0661(1)
15	0.0632(1)
20	0.0478(1)
24	0.0411(1)
32	0.0299(1)
48	0.0191(1)
64	0.0143(1)
80	0.0110(2)
100	0.0091(2)

within numerical errors, the value of the critical exponent reported in reference [53].

The scaling behavior can be further tested by plotting $R_{L,k}^X(p)$ vs. $(p - p_{c,k}) L^{\frac{1}{\nu}}$ and looking for data collapsing. Using the values of $p_{c,k}$ previously calculated and the value $\nu = 7/8$, an excellent scaling collapse was obtained (Fig. 5) for $R_{L,k}^I$ and all value of k -mer size. This leads to independent control and consistency check of numerical value of the critical exponent ν .

In order to bear out the universality class of the problem, the critical exponents β and γ were calculated from the scaling behavior of P and χ [3] as follows:

$$P = L^{-\beta/\nu} \overline{P} \left[|p - p_{c,k}| L^{1/\nu} \right], \quad (5)$$

and

$$\chi = L^{\gamma/\nu} \overline{\chi} \left[(p - p_{c,k}) L^{1/\nu} \right], \quad (6)$$

where \overline{P} and $\overline{\chi}$ are scaling functions for the respective quantities. According to equations (5) and (6), Figure 6 shows the excellent collapse of curves of P and χ (inset) for a typical k -mer size ($k = 5$) and different lattice sizes as indicated.

The data scaled extremely well using the reported percolation exponents $\beta = 0.41$ and $\gamma = 1.82$ [3]. The results obtained in Figures 5 and 6 suggest that the universality class corresponds to 3D percolation problem and clearly does not depend on the k -mer size. This kind of behavior has been observed in previous studies of percolation of extended objects. Thus, Cornette et al. [31] found that straight rigid k -mers and tortuous k -mers isotropically deposited on two-dimensional square lattices are in the same universality class as the standard percolation in two dimensions. The same result was obtained for percolation

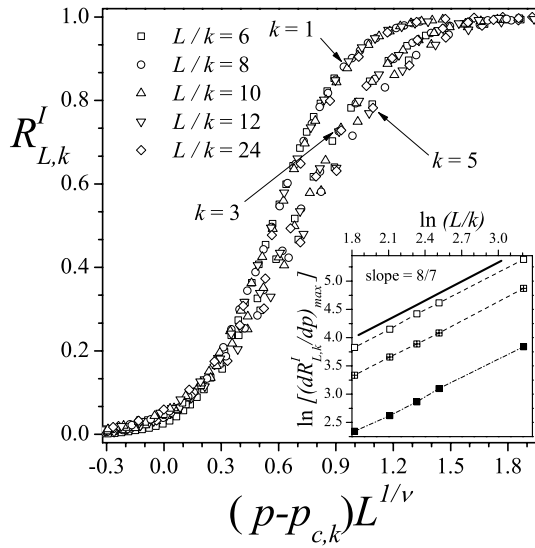


Fig. 5. Data collapse the fraction of percolation samples $R_{L,k}^I(p)$ as a function of the argument $(p - p_{c,k})L^{1/\nu}$. Each set of curves corresponds to different values of k as indicated. For each k , different lattice sizes ($L/k = 6, 8, 10, 12, 24$) have been considered. Inset: $\ln \left[\frac{d}{dp} (R_{L,k}^I)_{max} \right]$ as a function of $\ln(L/k)$ for different values of k as indicated. According to equation (4) the slope corresponds to $1/\nu$.

of aligned rigid rods [38] and percolation of rigid rods under equilibrium conditions [55] on two-dimensional square lattices. The authors reported that even though the intersection points of the curves of $R_{L,k}^X(p)$ for different system sizes exhibit nonuniversal critical behavior¹, the percolation transition occurring in the system belongs to the standard random percolation universality class regardless of the value of k considered.

4 Conclusions

In this paper, the percolation behavior of straight rigid k -mers deposited on a simple cubic lattice has been studied by numerical MC simulations and finite-size analysis.

For each value of k , the probability $R_{L,k}^X(p)$ that a system of linear size L percolates at concentration p was used to obtain the critical concentration $p_{c,k}$.

The plot of $p_{c,k}$ vs. k showed a monotonic decrease in all the studied k range. This result is quite surprising when compared with the results reported in reference [40], where a steep increase is shown after an initial low- k [$k \in (1, 13)$] decrease. This finding yields two possible conclusions: (a) the results reported by Tarasevich et al. in reference [40] are not applicable to the present system, (b) the utmost k value studied in the present work is not large enough to appreciate the reported behavior.

Finally, the analysis of the critical exponents ν , β and γ , supported by the excellent data collapse of the curves of $R_{L,k}^X(p)$, P and χ , strongly suggested that the

¹ The nonuniversality of the intersection points of the curves of $R_{L,k}^X(p)$ has also been observed for percolation of partially ordered k -mers [40].

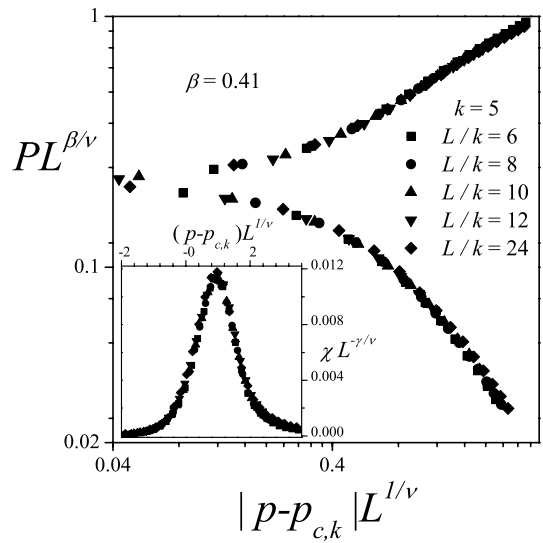


Fig. 6. Data collapse of the order parameter, $PL^{\beta/\nu}$ vs. $|p - p_{c,k}|L^{1/\nu}$, and of the susceptibility $\chi L^{-\gamma/\nu}$ vs. $(p - p_{c,k})L^{1/\nu}$ (inset) for $k = 5$. The plots were made using the percolation exponents $\nu = 7/8$, $\beta = 0.41$ and $\gamma = 1.82$.

percolation phase transition involved in the considered problem belongs to the same universality class of the ordinary 3D random percolation.

This work was supported in part by CONICET (Argentina) under project number PIP 112-200801-01332; Universidad Nacional de San Luis (Argentina) under project 322000; Universidad Tecnológica Nacional, Facultad Regional San Rafael, under project PID UTN 1475 Disp. 284/12; and the National Agency of Scientific and Technological Promotion (Argentina) under project PICT-2010-1466.

References

1. H. Kesten, *Percolation Theory for Mathematicians* (Birkhäuser, Boston, 1982)
2. R. Zallen, *The Physics of Amorphous Solids* (John Wiley & Sons, New York, 1983)
3. D. Stauffer, A. Aharony, *Introduction to Percolation Theory*, 2nd edn. (Taylor & Francis, London, 1985)
4. M. Sahimi, *Applications of Percolation Theory* (Taylor & Francis, London, 1994)
5. M. Sahimi, *Flow and transport in Porous Media and Fractured Rock* (VCH, Weinheim, 1995)
6. G. Grimmett, *Percolation* (Springer-Verlag, Berlin, 1999)
7. B. Bollobás, O. Riordan, *Percolation* (Cambridge University Press, New York, 2006)
8. Y. Gazit, D.A. Berk, M. Leunig, L.T. Baxter, R.K. Jain, *Phys. Rev. Lett.* **75**, 2428 (1995)
9. J.W. Baish, Y. Gazit, D.A. Berk, M. Nozue, L.T. Baxter, R.K. Jain, *Microvasc. Res.* **51**, 327 (1996)
10. D.S. Callaway, M.E.J. Newman, S.H. Strogatz, D.J. Watts, *Phys. Rev. Lett.* **85**, 5468 (2000)
11. S.N. Dorogovtsev, A.V. Goltsev, J.F.F. Mendes, *Rev. Mod. Phys.* **80**, 1275 (2008)
12. A. Bashan, R. Parshani, S. Havlin, *Phys. Rev. E* **83**, 051127 (2011)

13. R.K. Pan, M. Kivelä, J. Saramäki, K. Kaski, J. Kertész, Phys. Rev. E **83**, 046112 (2011)
14. A. Yazdi, H. Hamzeshpour, M. Sahimi, Phys. Rev. E **84**, 046317 (2011)
15. S. Kirkpatrick, Rev Mod. Phys. **45**, 574 (1973)
16. C. Moore, M.E.J. Newman, Phys. Rev. E **61**, 5678 (2000)
17. C.L. Henley, Phys. Rev. Lett. **71**, 2741 (1993)
18. N. Zekri, L. Zekri, C. Lallemand, Y. Pizzo, A. Kaiss, J.-P. Clerc, B. Porterie, J. Phys.: Conf. Ser. **395**, 012010 (2012)
19. E. Kenah, J.M. Robins, Phys. Rev. E **76**, 036113 (2007)
20. R. Cohen, K. Erez, D. ben-Avraham, S. Havlin, Phys. Rev. Lett. **85**, 4626 (2000)
21. M. Adam, M. Delsanti, D. Durand, G. Hild, J.P. Munch, Pure Appl. Chem. **53**, 1489 (1981)
22. Y. Chen, G. Paul, R. Cohen, S. Havlin, S. P. Borgatti, F. Liljeros, H.E. Stanley, Phys. Rev. E **75**, 046107 (2007)
23. S. Solomon, G. Weisbuch, L. de Arcangelis, N. Jan, D. Stauffer, Physica A **277**, 239 (2000)
24. C.M. Fortuin, P.W. Kasteleyn, Physica **57**, 536 (1972)
25. A. Coniglio, J. Phys.: Condens. Matter **13**, 9039 (2001)
26. S.R. Broadbent, J.M. Hammersley, Proc. Cambridge Phil. Soc. **53**, 629 (1957)
27. J.M. Hammersley, Proc. Cambridge Phil. Soc. **53**, 642 (1957)
28. H.L. Frisch, J.M. Hammersley, J. Soc. Ind. Appl. Math. **11**, 894 (1963)
29. P. Agrawal, S. Redner, P.J. Reynolds, H.E. Stanley, J. Phys. A **12**, 2073 (1979)
30. V. Cornette, A.J. Ramirez-Pastor, F. Nieto, Physica A **327**, 71 (2003)
31. V. Cornette, A.J. Ramirez-Pastor, F. Nieto, Eur. Phys. J. B **36**, 391 (2003)
32. V. Cornette, A.J. Ramirez-Pastor, F. Nieto, Phys. Lett. A **353**, 452 (2006)
33. V. Cornette, A.J. Ramirez-Pastor, F. Nieto, J. Chem. Phys. **125**, 204702 (2006)
34. V.A. Cherkasova, Y.Y. Tarasevich, N.I. Lebovka, N.V. Vygnitskii, Eur. Phys. J. B **74**, 205 (2010)
35. M. Dolz, F. Nieto, A.J. Ramirez-Pastor, Eur. Phys. J. B **43**, 363 (2005)
36. M. Dolz, F. Nieto, A.J. Ramirez-Pastor, Phys. Rev. E **72**, 066129 (2005)
37. M. Dolz, F. Nieto, A.J. Ramirez-Pastor, Physica A **374**, 239 (2007)
38. P. Longone, P.M. Centres, A.J. Ramirez-Pastor, Phys. Rev. E **85**, 011108 (2012)
39. Y.Y. Tarasevich, V.A. Cherkasova, Eur. Phys. J. B **60**, 97 (2007)
40. Y.Y. Tarasevich, N.I. Lebovka, V.V. Laptev, Phys. Rev. E **86**, 061116 (2012)
41. K. Binder, Rep. Prog. Phys. **60**, 488 (1997)
42. F. Yonezawa, S. Sakamoto, M. Hori, Phys. Rev. B **40**, 636 (1989)
43. F. Yonezawa, S. Sakamoto, M. Hori, Phys. Rev. B **40**, 650 (1989)
44. S. Biswas, A. Kundu, A.K. Chandra, Phys. Rev. E **83**, 021109 (2011)
45. A.K. Chandra, Phys. Rev. E **85**, 021149 (2012)
46. J. Hoshen, R. Kopelman, Phys. Rev. B **14**, 3438 (1976)
47. V. Privman, P.C. Hohenberg, A. Aharony, Universal Critical-Point Amplitude Relations, in *Phase Transitions and Critical Phenomena*, edited by C. Domb, J.L. Lebowitz (Academic, NY, 1991) Vol. 14, Chap. 1
48. M.E.J. Newman, R.M. Ziff, Phys. Rev. Lett. **85**, 4104 (2000)
49. S. Fortunato, Phys. Rev. B **67**, 014102 (2003)
50. S. Fortunato, Phys. Rev. B **66**, 054107 (2002)
51. W. Selke, L.N. Shchur, J. Phys. A **38**, L739 (2005)
52. W. Selke, J. Stat. Mech.: Theory Exp. **2007**, P04008 (2007)
53. A. Bunde, S. Havlin, *Fractals and Disordered Systems* (Springer, Heidelberg, 1996)
54. Y. Deng, H.W.J. Blöte, Phys. Rev. E **72**, 016126 (2005)
55. D.A. Matoz-Fernandez, D.H. Linares, A.J. Ramirez-Pastor, Eur. Phys. J. B **85**, 296 (2012)